NeuroImage 88 (2014) 155–161

Contents lists available at ScienceDirect

NeuroImage

journal homepage: www.elsevier.com/locate/ynimg

Polarity-specific effects of motor transcranial direct current stimulation on fMRI resting state networks

Ugwechi Amadi [a], Andrei Ilie [a,b], Heidi Johansen-Berg [a], Charlotte Jane Stagg [a,*]

[a] Oxford Centre for Functional MRI of the Brain (FMRIB), Nuffield Department of Clinical Neurosciences, University of Oxford, Oxford, UK
[b] Department of Pharmacology, University of Oxford, Oxford, UK

ARTICLE INFO

Article history:
Accepted 18 November 2013
Available online 25 November 2013

Keywords:
Transcranial direct current stimulation
Resting state connectivity
Functional MRI
Independent component analysis
Motor
Default mode

ABSTRACT

Transcranial direct current stimulation (tDCS) has been used to modify motor performance in healthy and patient populations. However, our understanding of the large-scale neuroplastic changes that support such behavioural effects is limited. Here, we used both seed-based and independent component analyses (ICA) approaches to probe tDCS-induced modifications in resting state activity with the aim of establishing the effects of tDCS applied to the primary motor cortex (M1) on both motor and non-motor networks within the brain. Subjects participated in three separate sessions, during which resting fMRI scans were acquired before and after 10 min of 1 mA anodal, cathodal, or sham tDCS. Cathodal tDCS increased the inter-hemispheric coherence of resting fMRI signal between the left and right supplementary motor area (SMA), and between the left and right hand areas of M1. A similar trend was documented for the premotor cortex (PMC). Increased functional connectivity following cathodal tDCS was apparent within the ICA-generated motor and default mode networks. Additionally, the overall strength of the default mode network was increased. Neither anodal nor sham tDCS produced significant changes in resting state connectivity. This work indicates that cathodal tDCS to M1 affects the motor network at rest. In addition, the effects of cathodal tDCS on the default mode network support the hypothesis that diminished top-down control may contribute to the impaired motor performance induced by cathodal tDCS.

Introduction

Non-invasive neuromodulatory techniques have attracted increasing interest over recent years as putative therapies for the treatment of a variety of disorders including epilepsy, stroke, Parkinson's disease, and chronic pain (see Brunoni et al., 2012; Fregni and Pascual-Leone, 2007; Hummel and Cohen, 2006 for reviews). Of these, transcranial direct current stimulation (tDCS) shows perhaps the most promise as a potential clinical tool. However, currently the use of tDCS is limited by an incomplete understanding of the exact mechanisms by which tDCS affects brain function.

tDCS relies on the passage of a low-amplitude constant electric current between two electrodes placed on the scalp. tDCS applied to the primary motor cortex (M1) affects the activity of the underlying cortex in a polarity-specific manner (Nitsche and Paulus, 2000). While studies have investigated the effects of tDCS applied to M1 on closely anatomically connected regions (Lang et al., 2005; Stagg et al., 2009b) it is still not clear to what extent M1 stimulation modulates activity in the remainder of the motor network at rest.

The organization and functional connectivity of brain networks can be investigated using resting state functional MRI. First established by Biswal and colleagues in 1995, this technique examines low frequency fluctuations (generally <0.1 Hz) of the BOLD signal which occur in the brain in the absence of task performance (Biswal et al., 1995). Temporally correlated fluctuations in resting BOLD signal between regions are commonly considered to reflect underlying functional connectivity, with an increased correlation in activity reflecting increased connectivity (Fox and Raichle, 2007).

Previous studies investigating the effects of motor tDCS paradigms that would be expected to induce lasting after-effects on functional connectivity have demonstrated that anodal tDCS increases local functional connectivity *within* M1 (Polanía et al., 2012a; Sehm et al., 2013). Anodal tDCS to M1 has also been shown to increase resting activity *between* pre-defined key nodes in the motor network, such as M1 and thalamus (Polanía et al., 2012b). Studies have additionally investigated the effects of tDCS across the whole brain revealing regions showing increased coupling with the rest of the brain both within and beyond the motor system (Polanía et al., 2011; Sehm et al., 2012). These results clearly demonstrate that local application of tDCS can have widespread effects. However, the methods chosen do not allow for testing of whether the

* Corresponding author at: FMRIB, John Radcliffe Hospital, Headington, Oxford, OX3 9DU, UK. Fax: +44 1865 222717.
E-mail address: charlotte.stagg@ndcn.ox.ac.uk (C.J. Stagg).

1053-8119
http://dx.doi.org/10.1016/j.neuroimage.2013.11.037

regions showing effects were functionally connected with one another, an important question when understanding the behavioural effects of tDCS.

An alternative, network-based, approach to the analysis of functional connectivity changes across the whole brain is independent component analysis (ICA) (Beckmann et al., 2005). ICA is a model-free method that decomposes data into spatial and temporal components. When applied to resting fMRI data it identifies brain regions with similar resting BOLD signal timecourses. A typical ICA output from fMRI data acquired at rest is a set of canonical networks representing various cognitive and sensory domains (Beckmann et al., 2005), that are both behaviourally (Smith et al., 2009) and clinically relevant (Rosazza and Minati, 2011). Previously, ICA has been used to examine how tDCS to the dorsolateral prefrontal cortex affects resting state fMRI networks (Keeser et al., 2011; Peña-Gómez et al., 2012; Stagg et al., 2013). However, to date there have been no studies examining the effects of M1 tDCS on such networks. A study by Venkatakrishnan and colleagues used ICA to investigate the effects of M1 tDCS on resting state MEG activity, but did not look within any of the previously described canonical resting state networks, and found no difference between anodal and cathodal stimulation (Venkatakrishnan et al., 2011).

The present study expands on previous work with the aim of understanding how M1 tDCS affects underlying brain connectivity by analysing resting state fMRI using two complementary methodologies. First, we used an ROI-based correlation approach to assess inter-hemispheric interactions between regions within the motor system. We then explored functional changes in ICA-generated networks, with regard to overall strength and connectivity. Performing these analyses with both anodal and cathodal tDCS allows for tentative investigation into how different effects on resting activity may give rise to the opposing behavioural results generated by the two polarities.

Materials and methods

Subjects

Eleven healthy, right-handed subjects (mean age 22.9 years [range 21–24], 7 female) participated in this study. All participants gave their written informed consent in accordance with local ethics committee approval. Due to personal reasons one subject completed the cathodal and sham, but not anodal, sessions.

Overview

Subjects participated in three sessions, during which they received either anodal, cathodal, or sham tDCS in the scanner. Prior to and immediately following tDCS, 10 min of resting state fMRI data were acquired, during which subjects were instructed to relax and keep their eyes closed. During the sham tDCS session, subjects performed a motor task following the final resting state scan. The order of the sessions was counterbalanced across the group. Experimental sessions were separated by at least 48 h and real tDCS sessions by at least 1 week. Subjects were blind to the type of stimulation they received in any session.

tDCS administration

Prior to entering the scanner tDCS electrodes were fitted to the participant's scalp. The electrodes measured 5 × 7 cm, and were fitted with 5 kΩ resistors to be compatible with a magnetic field. The stimulating electrode was centred over the dominant (left) M1, as measured to be 5 cm lateral to Cz. The reference electrode was placed over the right supraorbital ridge. Both electrodes were affixed to the scalp using high chloride EEG paste as a conducting medium (Eldith, Germany). Subjects were positioned in the scanner as described previously (Stagg et al., 2009a). tDCS was delivered using a DC stimulator (Magstim Eldith, Germany). A 1 mA current was applied for 10 min (10 s fade in/fade out). For the sham condition, the current was ramped up over 10 s and then turned off.

Functional ROI definition

At the end of the sham stimulation session, subjects performed a visually-cued explicit motor sequence learning task described in detail elsewhere (see Stagg et al., 2011a for details), while EPI data were acquired. In brief, the task consisted of sequence blocks that comprised three repeats of a ten-digit sequence that subjects learned explicitly. This served as a localizer for motor activation, which was subsequently used to define functional ROIs of motor areas (see the section 'ROI-based analysis').

Image acquisition

All MR data were acquired on a 3 T Varian Scanner. In brief, two resting state scans and a field map were acquired during each session. 10 min of axial echo-planar volumes were acquired during at rest before and immediately after tDCS using a 4 channel head coil (TR = 3000 ms, TE = 28 ms, FOV = 192 × 192). During the sham session, additional EPI data were acquired while the subject performed the behavioural task described in the section 'Functional ROI definition', using the same sequence parameters. One 1 mm isotropic T1-weighted scan was also acquired for registration purposes using a 3D Turbo Flash sequence (TR = 13 ms, TE = 4.9 ms, flip angle = 8, FOV = 256 × 256).

Image analysis

Image pre-processing

All image analysis steps were performed using tools from the FMRIB Software Library (FSL, www.fmrib.ox.ac.uk/fsl) (Jenkinson et al., 2012; Smith et al., 2004; Woolrich et al., 2009). Prior to statistical analysis the following pre-processing steps were applied: motion correction using MCFLIRT (Jenkinson et al., 2002); B0 unwarping with field maps using FUGUE; spatial smoothing with a Gaussian kernel of 6 mm; and highpass temporal filtering at 150 s to remove low frequency artefacts. Registration to individual T1-weighted structural images and then to standard MNI space was performed via linear and then non-linear registration using FLIRT and FNIRT within FSL (Jenkinson and Smith, 2001).

ROI-based analysis

We defined our functional ROIs in two stages. First, anatomical ROIs were defined for the primary motor cortex (M1), hand area of the M1, premotor cortex (PMC) and supplementary motor area (SMA) as follows, to provide anatomical limits for our functional ROIs:

- M1 Lateral and medial half of the anterior bank of the central sulcus, extending from the dorsal surface of the lateral ventricles to the top of the brain.
- Hand area of M1 (M1Hand) The knob of the precentral gyrus, posterior to the junction of the superior frontal sulcus with the precentral sulcus.
- PMC Precentral gyrus and precentral sulcus, extending from the dorsal surface of the lateral ventricles to the top of the brain.
- SMA The medial surface of the brain above the cingulate sulcus, posterior to the vertical plane above the anterior commissure (VCA line) and anterior to the vertical plane above the posterior commissure (VCP line).

Then, functionally defined motor regions of interest were created from the EPI images acquired during performance of the motor learning task following the sham stimulation session. The task EPI data was pre-

processed as outlined above. Statistical analysis was carried out using FILM with local autocorrelation correction (Woolrich et al., 2001). FEAT was used to create activation maps for each individual, using as a regressor a square waveform convolved with the haemodynamic response function to model the on–off periods of task performance (Beckmann et al., 2003). The resulting Z statistic images depicting positive correlations to this function were thresholded at $Z > 2.0$ and a corrected cluster extent threshold of $p < 0.01$. For each pre-defined anatomical region, functional ROI masks were created for each subject by dilating the maximally active voxel within each anatomical ROI to produce a cuboid ROI of $8 \times 8 \times 8$ mm centred on the peak voxel. As the task-induced activation was primarily left lateralized, functional ROI masks were created for the left hemispheric ROIs, then flipped about the y-axis to create right hemispheric ROIs (Inline Supplementary Table S1).

Inline Supplementary Table S1 can be found online at http://dx.doi.org/10.1016/j.neuroimage.2013.11.037.

Using as masks the functionally defined ROIs for M1, the hand area, PMC, and SMA, the timecourse of the resting BOLD signal was extracted from each subject's images for each stimulation condition (i.e., anodal, cathodal and sham) and timepoint (i.e., pre- and post-stimulation). The resulting timecourses were then correlated between hemispheres for each ROI (e.g., left-M1 with right-M1), to give a measure of inter-hemispheric functional connectivity. As Pearson's r is not normally distributed the resulting r values were transformed into Z scores using the Fisher r-to-Z transformation. Statistical analyses, including repeated measures ANOVAs (RM-ANOVAs) and post-hoc paired t-tests were carried out in SPSS (IBM, version 19.0.0).

Independent component analysis

Pre-processed resting state scans were analysed using an independent component analysis approach (ICA), as implemented in MELODIC (Beckmann and Smith, 2004). Initially, all scans from all sessions were combined and run in a group ICA using the temporal concatenation method within MELODIC, constrained to identify 25 components. The appropriate number of components was calculated based on an initial analysis of the population using model order estimation (Beckmann and Smith, 2004).

Networks, including the DMN, were identified using an automated approach by calculating the spatial correlation between each component and the standard masks of the canonical networks, as described previously (Beckmann et al., 2005). The component with the highest anatomical similarity to each network was then chosen. A dual-regression approach (Filippini et al., 2009) was then taken as follows: group-defined RSNs were used as a regressor in separate GLM analyses to extract a timeseries of the BOLD signal from the EPI data from each subject and each session independently. Each individual timeseries was then used in a second GLM to extract the spatial maps that corresponded to each RSN timecourse for each subject and session separately.

Permutation-based statistics were run on these individually defined resting networks, using RANDOMISE (Nichols and Holmes, 2002) as implemented within FSL to create within and between condition activation maps for each network. The resulting t-statistic images were thresholded using cluster-based thresholding corrected for multiple comparisons at $t > 2.0$,and $p < 0.05$.

Additionally, the mean resting BOLD signal was extracted from each of the binarized MELODIC-defined resting networks to determine their overall strength.

Results

Cathodal tDCS increases the coherence of resting motor activity between hemispheres

We first investigated whether M1 tDCS caused changes in resting BOLD signal in motor cortical areas. We specifically examined the M1, the hand area of M1 ($M1_{Hand}$), SMA, and PMC of the left and right hemispheres.

Correlations in the timeseries of resting activity between the left and right M1, $M1_{Hand}$, SMA, and PMC were determined for each subject, before and after each type of stimulation (Fig. 1). For statistical analysis, the resulting Z scores were entered into a RM-ANOVA with one factor of ROI (M1, $M1_{Hand}$, PMC, SMA), one factor of Stimulation type ("Stim"; anodal, cathodal and sham) and one factor of Time (pre- and post-stimulation). There was a significant ROI × Stim × Time interaction ($F(4,36) = 3.319$, $p = 0.021$). To determine what was driving this three-way interaction, separate RM-ANOVAs were performed for anodal or cathodal stimulation versus sham and then for each ROI separately.

When comparing anodal to sham stimulation for each ROI, there were no significant interactions (all $p > 0.05$). When comparing cathodal to sham, there was a significant ROI × Stim × Time interaction ($F(2,20) = 4.001$, $p = 0.035$). To determine in which ROIs these effects were occurring, RM-ANOVAs were then performed for each ROI separately. There was a significant Stim × Time interaction for both the $M1_{Hand}$ and the SMA ($M1_{Hand}$: $F(1,10) = 9.874$, $p = 0.010$; SMA: $F(1,10) = 9.041$, $p = 0.013$). T-tests comparing the strength of the correlations between the left and right hand area, and left and right SMA before and after cathodal stimulation demonstrated a significant increase in inter-hemispheric connectivity in both regions after cathodal stimulation ($M1_{Hand}$: $t(10) = 4.591$, $p = 0.001$; SMA: $t(10) = 2.874$, $p = 0.017$). In addition, a trend toward a significant increase in inter-hemispheric connectivity following cathodal tDCS was found for the PMC ($t(10) = 2.123$, $p = 0.060$; Fig. 1).

To ensure that these tDCS-induced changes in inter-hemispheric connectivity were not driven by baseline differences between the scans, we performed a repeated-measures ANOVA for the pre-stimulation scans for each ROI separately. No significant main effect of stimulation was seen for the pre-scans for any of the ROIs (M1 ($F(2,18) = 0.58$, $p = 0.57$), $M1_{Hand}$ ($F(2,18) = 0.06$, $p = 0.95$), SMA ($F(2,18) = 2.14$.$p = 0.15$), or PMC ($F2,18) = 1.57$, $p = 0.23$).

Cathodal tDCS increases the overall strength of the default mode network

These results suggest that cathodal tDCS to M1 affects connectivity within the motor network by increasing the functional inter-hemispheric connectivity between important network nodes such as $M1_{Hand}$ and SMA. To explore how tDCS affects functional connectivity across the whole brain we next used ICA to identify the canonical resting state networks and tested the effects of tDCS on the strength and connectivity within these networks.

Using an ICA approach eight resting state networks were identified that corresponded to the canonical motor, default mode, medial visual, lateral visual, executive control, auditory, right dorsal visual stream, and left dorsal visual stream RSNs previously described (Beckmann et al., 2005) (Fig. 2).

We first tested whether tDCS modified the overall strength of resting state networks. The mean resting activity in each of the eight identified networks was compared before and after each period of stimulation. A RM-ANOVA (RSN × Stim × Time) found an RSN × Stim interaction ($F(14,126) = 1.860$, $p = 0.037$), suggesting that the effects of stimulation varied between RSNs. Subsequent RM-ANOVAs comparing anodal to sham and cathodal to sham were run for each RSN. There was no significant effect of tDCS on any network when comparing anodal to sham (all $p > 0.05$). When comparing cathodal to sham, the only RSN where there was a significant effect of tDCS was the default mode network (DMN), which showed a Stim × Time interaction ($F(1,10) = 5.977$, $p = 0.035$). Paired t-tests on the mean DMN strength before and after stimulation demonstrated a significant increase in resting activity following cathodal tDCS ($t(9) = 3.046$, $p = 0.012$), but not following anodal or sham tDCS (anodal: $t(9) = 1.543$, $p = 0.157$; sham: $t(10) = 0.725$, $p = 0.485$) (Fig. 3A). As we had an *a priori* hypothesis

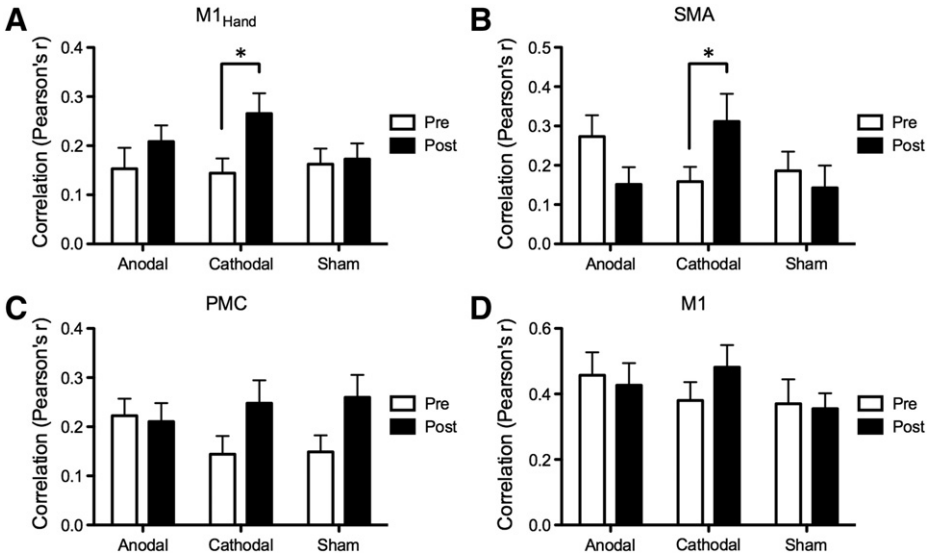

Fig. 1. Inter-hemispheric coherence within key motor network nodes. Cathodal stimulation increases inter-hemispheric coherence between specific regions within the motor network. (A) Significantly increased coherence was identified between the hand areas of the left and right M1 ($M1_{Hand}$) and (B) the left and right SMA. (C) A trend towards an increase in inter-hemispheric coherence after cathodal tDCS was also observed in the PMC. (D) No significant changes in inter-hemispheric coherence were observed for M1 as a whole. Error bars: ±1 SEM.

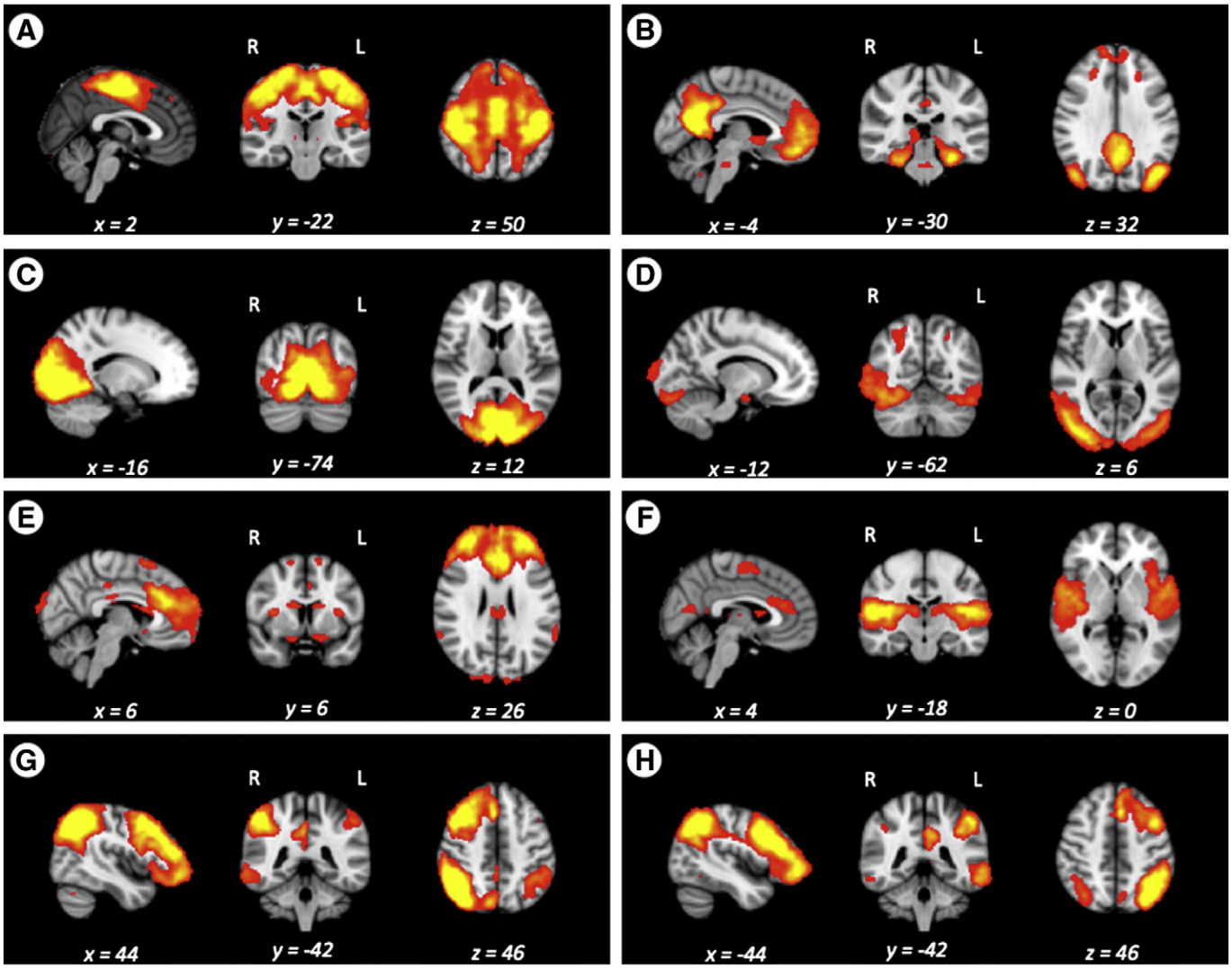

Fig. 2. The resting state networks. Melodic ICA generated resting state networks from our data. Group mean (A) motor, (B) default mode, (C) medial visual, (D) lateral visual, (E) executive, (F) auditory, (G) right dorsal visual stream, and (H) left dorsal visual stream networks.

for the effects of tDCS on the motor network, although no significant effects of tDCS were identified on resting activity changes within the motor network in the RM-ANOVA, we investigated polarity-specific effects within this network. This analysis revealed a trend toward increased resting activity following anodal stimulation (anodal: $t(9) = 1.993$, $p = 0.077$; cathodal: $t(10) = 1.401$, $p = 0.191$; sham: $t(10) = 0.221$, $p = 0.830$). The results of this exploratory analysis are shown in Fig. 3B.

Cathodal tDCS increases connectivity within the motor and default mode networks

Positing that stimulation may increase connectivity between specific areas of the resting state networks in addition to (or independent of) affecting the overall strength of the network, we ran an exploratory voxel-wise whole brain analysis comparing pre- and post-stimulation resting activity in the motor and default mode networks for each stimulation type. Cathodal stimulation led to significant increases in connectivity for specific clusters within both the motor (Fig. 4A) and default mode networks (Fig. 4B). No significant changes were found for equivalent whole brain analyses of anodal or sham stimulation. To explore the anatomical distribution of these network-specific changes in functional connectivity induced by cathodal tDCS we plotted the network strength from the clusters that showed significant changes due to cathodal stimulation (as plotted in Figs. 4A and B) for all three stimulation conditions (Figs. 4C and D). There was no evidence for change in network strength within these clusters following anodal or sham stimulation.

Discussion

This study was performed to investigate how tDCS affects brain connectivity at rest. We have demonstrated that cathodal tDCS applied to the primary motor cortex (M1) modulates resting state activity in a network-specific manner. Region of interest analyses probing the coherence of inter-hemispheric activity in major nodes within the motor network (M1, $M1_{Hand}$, SMA, and PMC) found increased inter-hemispheric connectivity between the $M1_{Hand}$ regions and the SMAs following cathodal tDCS. An ICA analysis identified the canonical resting state networks and found that cathodal tDCS increased the overall strength of the default mode network (DMN), and increased functional connectivity in specific regions within both the DMN and the motor network. There was a trend towards an increase in strength of the motor network with anodal tDCS, but this did not reach statistical significance.

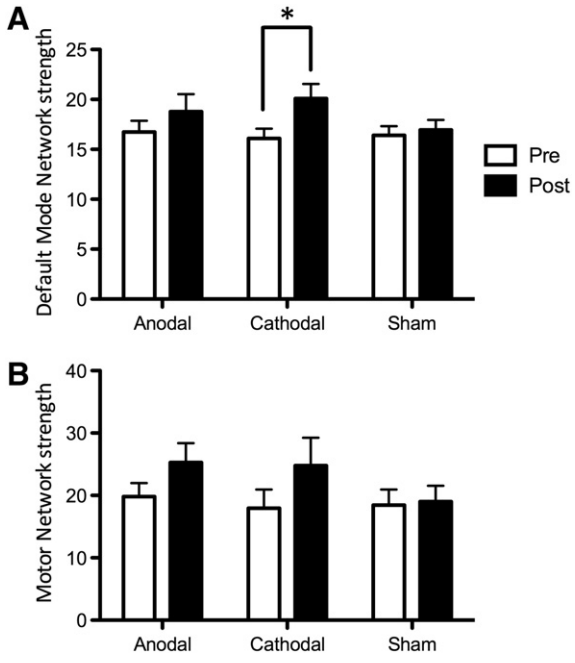

Fig. 3. Changes in network strength with tDCS. Cathodal tDCS increased the strength of the default mode network. (A) A significant ($p < 0.05$) increase in functional connectivity in the DMN was observed following cathodal, but not anodal or sham, tDCS. (B) The strength of the motor network was not significantly changed over time by tDCS. Error bars: ±1 SEM.

Though the overall strength of the motor network was not significantly modulated by tDCS, our ROI analysis revealed increased inter-hemispheric functional connectivity within major network nodes following cathodal tDCS. Specifically, we found an increase in coherence between the left and right hand areas of M1 and between the left and right SMA following cathodal tDCS. This is in line with a previous study which has found that cathodal tDCS increased local connectivity within the hand area of the primary motor cortex, but not globally across M1 (Polanía et al., 2012a).

It has been proposed that such modifications in connectivity and synchronization are the result of changes in the signal to noise ratio (Polanía et al., 2012a). At a cellular level cathodal tDCS causes neuronal hyperpolarization and decreased spontaneous firing within the stimulated region (Bindman et al., 1964), effectively decreasing local neuronal noise (Antal et al., 2004). This would result in increased signal to noise ratio within the stimulated area, promoting better communication with other regions and increasing synchronization (Polanía et al., 2011).

The link between resting connectivity and task-related activity is not necessarily clear. However, detrimental behavioural effects are seen on unimanual motor learning tasks performed *after* cathodal tDCS (Stagg et al., 2011b, 2012) and it may be that the changes in resting state connectivity seen here can begin to elucidate the mechanisms underlying this behavioural phenomenon. Unimanual movements recruit contralateral motor areas, with ipsilateral signals effectively treated as noise (Cincotta and Ziemann, 2008). During unimanual task performance, contralateral motor regions are positively modulated, while ipsilateral areas are inhibited (Grefkes et al., 2008). The increased signal from contralateral areas, combined with decreased noise from ipsilateral areas, results in improved efferent signal to noise ratio from the contralateral motor area. This may lead to more efficient synaptic transmission and, ultimately, faster motor execution (Grefkes et al., 2008). Cathodal tDCS, by synchronizing activity between the hand areas of the two hemispheres, may interfere with the ability of intrinsic mechanisms to perform this inter-hemispheric decoupling, resulting in impaired motor performance.

Previous work also suggests that the SMAs, and to a lesser extent the PMCs, mediate these inter-hemispheric interactions, modulating M1 activity in favour of the hemisphere responsible for the unimanual movement (Grefkes et al., 2008). Our study documented increased coherence in activity in the SMAs following cathodal tDCS, and a similar trend in the PMCs. This may reflect the SMA of both hemispheres working in concert to promote activity within both motor cortices, rather than the contralateral cortex exclusively.

Our findings also report an unexpected increase in strength of the DMN following cathodal tDCS. The DMN is thought to underlie processes necessary for passive cognitive states, such as introspection and "mind wandering" (Broyd et al., 2009; Rosazza and Minati, 2011). In line with this, and in contrast with other RSNs, key nodes within the DMN tend to exhibit increased activity during rest and decreased activity during task performance (Raichle et al., 2001). As such, it has been labelled as a task-negative network, the deactivation of which allows task-positive networks to more effectively facilitate task performance (Peña-Gómez et al., 2012). Indeed, increases in DMN activity have been shown to precede and predict worsened performance on behavioural tasks (Eichele et al., 2008; Li et al., 2007; Weissman et al., 2006). The default mode interference hypothesis proposes that over-activity of the task-negative component of the DMN results in attentional lapses during goal-directed actions, increasing error rates (Mason et al., 2007; Sonuga-Barke and Castellanos, 2007).

Studies investigating the effects of motor tDCS have found that cathodal tDCS impairs motor performance (Rosenkranz et al., 2000;

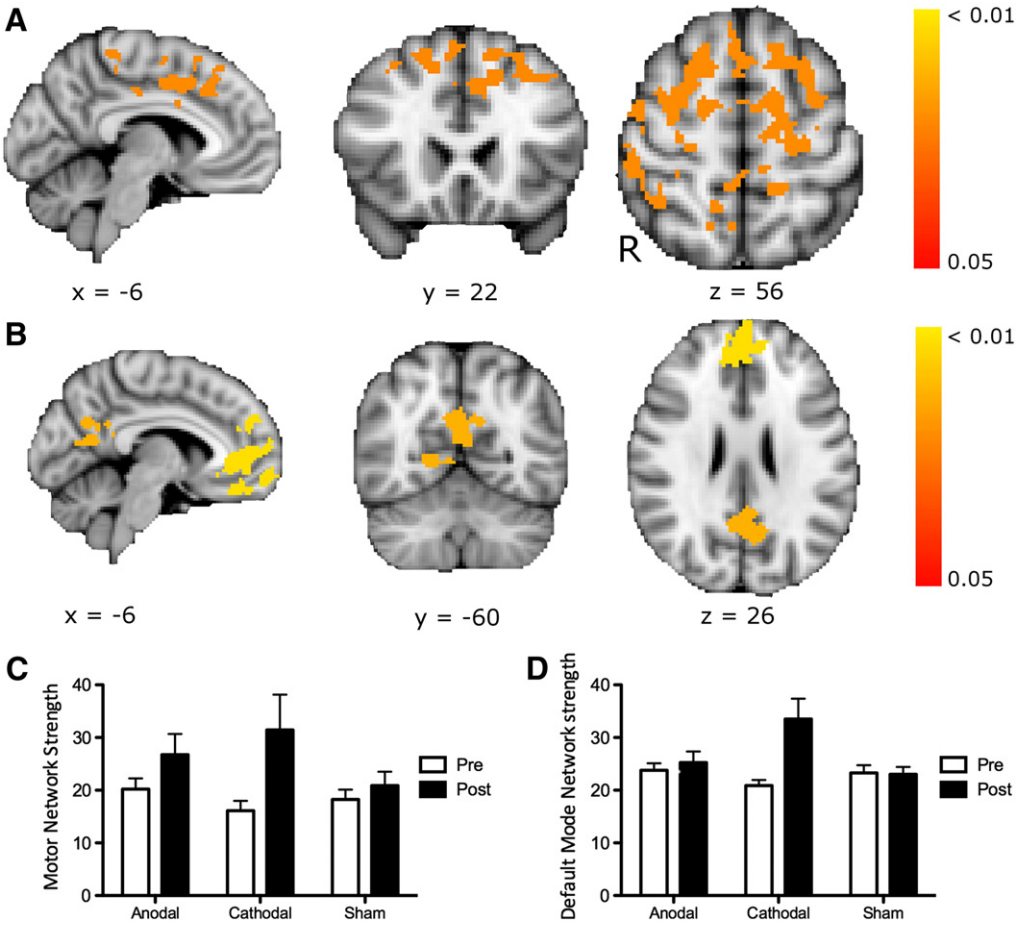

Fig. 4. Exploratory voxel-wise analysis of cathodal tDCS-induced changes in network strength. Cathodal stimulation modifies connectivity between specific areas of the motor and default mode networks. (A) Regions of increased functional connectivity within the motor network after cathodal tDCS. A single large cluster is identified. (B) Regions of increased functional connectivity within the DMN after cathodal tDCS. A further exploratory analysis investigated changes in functional connectivity within these identified regions for the motor network (C) and the default mode network (D). No significant modulation of functional connectivity was identified within these regions after anodal or sham stimulation. Bar graphs represent the amount of resting activity in the clusters shown. Error bars: ±1 SEM.

Stagg et al., 2011b, 2012). Taken together, these results suggest that cathodal tDCS may worsen motor performance via the DMN in two complementary ways. Firstly, increased task-negative activity might interfere with the ability of task-positive networks to execute the behavioural task. Secondly, impaired top-down control caused by increased DMN strength may result in more attentional lapses, contributing to the reduction in motor learning apparent during cathodal stimulation.

We found a trend towards increased functional connectivity within the motor network following anodal tDCS, consistent with the idea that anodal tDCS may decrease local inhibition (Nitsche et al., 2005; Stagg et al., 2009a) and increase local neuronal activity (Nitsche and Paulus, 2000). However, other comparisons did not produce evidence for changes in network-level resting state activity when probing the effects of anodal tDCS. These results contrast with previous findings of *decrease* in functional connectivity in cortico-cortical connections following anodal tDCS to M1 (Polanía et al., 2011), and an *increase* in functional connectivity in thalamo-cortical circuits, after anodal tDCS to M1 (Polanía et al., 2012b).

The lack of consensus as to the effects of tDCS on resting state connectivity is striking. This may be due to experimental differences between studies such as differences in tDCS protocols, fMRI acquisition parameters, or the attentional state of the subjects (eyes open/eyes closed). However, it is also important to note that different analysis approaches may be differentially sensitive to aspects of functional connectivity change. The current study differs from previous work in its use of a network-based approach, and in its sole use of cortical ROIs, meaning that it is likely to be differently sensitive from previous work. The differentially sensitive nature of the analysis approaches is highlighted most clearly by the work of Sehm and colleagues, who found widespread functional connectivity effects of anodal tDCS in the same montage as used here when using a graph-theory based approach (Sehm et al., 2012), but not when using a seed-based analysis (Sehm et al., 2013).

It is also possible that greater power to detect effects of anodal tDCS could be achieved through a larger sample, though we believe this is unlikely as we did find robust and significant effects of cathodal tDCS with the group studied here, and the within-subject design of our experiment added to its sensitivity.

As with the majority of tDCS experiments, in this study we have utilised an electrode montage which means that anodal tDCS to M1 simultaneously delivers cathodal stimulation to the prefrontal cortex, and *vice versa* for cathodal tDCS. Because the DMN partially encompasses the PFC, it is not possible to be sure whether the increased strength of the DMN after cathodal tDCS to M1 is a result of M1 stimulation specifically, or if it was driven by anodal stimulation of the PFC. A recent behavioural study has suggested that there may be possible functional effects of the reference electrode (Kaminski et al., 2013), and future studies using alternative electrode configurations could help to determine whether the reference electrode is, at least in part, driving the effects observed here.

Conclusions

In the present study, we examined stimulation-induced modulation of resting functional network connectivity. Cathodal tDCS induced

increased functional connectivity within the default mode and motor resting state networks. Such results suggest that cathodal tDCS may worsen motor learning via at least two mechanisms. Firstly, increased DMN activity and connectivity may impair top-down control. Secondly, increased inter-hemispheric connectivity between bilateral SMA and PMC may interfere with the natural, facilitatory inter-hemispheric decoupling of motor regions necessary for performing unimanual motor tasks. Future studies may probe these potential explanations by combining resting state imaging with task-based paradigms.

Acknowledgments

The research was supported by the National Institute for Health Research (NIHR) Oxford Biomedical Research Centre based at Oxford University Hospitals NHS Trust and University of Oxford. The views expressed are those of the authors and not necessarily those of the NHS, the NIHR, or the Department of Health. We also acknowledge support of the Wellcome Trust (HJB) and the MRC (HJB). Core support to the FMRIB Centre is provided by the MRC. UA is grateful to the Rhodes Trust for support.

References

Antal, A., Nitsche, M.A., Kruse, W., Kincses, T.Z., Hoffmann, K.-P., Paulus, W., 2004. Direct current stimulation over V5 enhances visuomotor coordination by improving motion perception in humans. J. Cogn. Neurosci. 16, 521–527.

Beckmann, C., Smith, S., 2004. Probabilistic independent component analysis for functional magnetic resonance imaging. IEEE Trans. Med. Imaging 23, 137–152.

Beckmann, C.F., DeLuca, M., Devlin, J.T., Smith, S.M., 2005. Investigations into resting-state connectivity using independent component analysis. Philos. Trans. R. Soc. Lond. B Biol. Sci. 360, 1001–1013.

Beckmann, C.F., Jenkinson, M., Smith, S.M., 2003. General multilevel linear modeling for group analysis in FMRI. NeuroImage 20, 1052–1063.

Bindman, L., Lippold, O.C., Redfearn, J.W., 1964. The action of brief polarizing currents on the cerebral cortex of the rat (1) during current flow and (2) in the production of long-lasting after-effects. J. Physiol. Lond. 172, 369–382.

Biswal, B., Yetkin, F.Z., Haughton, V.M., Hyde, J.S., 1995. Functional connectivity in the motor cortex of resting human brain using echo-planar MRI. Magn. Reson. Med. 34, 537–541.

Broyd, S.J., Demanuele, C., Debener, S., Helps, S.K., James, C.J., Sonuga-Barke, E.J.S., 2009. Default-mode brain dysfunction in mental disorders: a systematic review. Neurosci. Biobehav. Rev. 33, 279–296.

Brunoni, A.R., Nitsche, M.A., Bolognini, N., Bikson, M., Wagner, T., Merabet, L., Edwards, D.J., Valero-Cabre, A., Rotenberg, A., Pascual-Leone, A., Ferrucci, R., Priori, A., Boggio, P.S., Fregni, F., 2012. Clinical research with transcranial direct current stimulation (tDCS): challenges and future directions. Brain Stimul. 5, 175–195.

Cincotta, M., Ziemann, U., 2008. Neurophysiology of unimanual motor control and mirror movements. Clin. Neurophysiol. 119, 744–762.

Eichele, T., Debener, S., Calhoun, V.D., Specht, K., Engel, A.K., Hugdahl, K., von Cramon, D.Y., Ullsperger, M., 2008. Prediction of human errors by maladaptive changes in event-related brain networks. Proc. Natl. Acad. Sci. U. S. A. 105, 6173–6178.

Filippini, N., MacIntosh, B.J., Hough, M.G., Goodwin, G.M., Frisoni, G.B., Smith, S.M., Matthews, P.M., Beckmann, C.F., Mackay, C.E., 2009. Distinct patterns of brain activity in young carriers of the APOE-epsilon4 allele. Proc. Natl. Acad. Sci. U. S. A. 106, 7209–7214.

Fox, M.D., Raichle, M.E., 2007. Spontaneous fluctuations in brain activity observed with functional magnetic resonance imaging. Nat. Rev. Neurosci. 8, 700–711.

Fregni, F., Pascual-Leone, A., 2007. Technology insight: noninvasive brain stimulation in neurology—perspectives on the therapeutic potential of rTMS and tDCS. Nat. Clin. Pract. Neurol. 3, 383–393.

Grefkes, C., Eickhoff, S.B., Nowak, D.A., Dafotakis, M., Fink, G.R., 2008. Dynamic intra- and interhemispheric interactions during unilateral and bilateral hand movements assessed with fMRI and DCM. NeuroImage 41, 1382–1394.

Hummel, F.C., Cohen, L.G., 2006. Non-invasive brain stimulation: a new strategy to improve neurorehabilitation after stroke? Lancet Neurol 5, 708–712.

Jenkinson, M., Bannister, P., Brady, M., Smith, S., 2002. Improved optimization for the robust and accurate linear registration and motion correction of brain images. NeuroImage 17, 825–841.

Jenkinson, M., Smith, S.M., 2001. A global optimisation method for robust affine registration of brain images. Med. Image Anal. 5, 143–156.

Jenkinson, M.M., Beckmann, C.F.C., Behrens, T.E.J.T., Woolrich, M.W.M., Smith, S.M.S., 2012. FSL. NeuroImage 62, 782–790.

Kaminski, E., Hoff, M., Sehm, B., Taubert, M., Conde, V., Steele, C.J., Villringer, A., Ragert, P., 2013. Neuroscience letters. Neurosci. Lett. 552, 76–80.

Keeser, D., Meindl, T., Bor, J., Palm, U., Pogarell, O., Mulert, C., Brunelin, J., Moller, H.-J., Reiser, M., Padberg, F., 2011. Prefrontal transcranial direct current stimulation changes connectivity of resting-state networks during fMRI. J. Neurosci. 31, 15284–15293.

Lang, N., Siebner, H., Ward, N., Lee, L., Nitsche, M., Paulus, W., Rothwellt, J.C., Lemon, R., Frackowiak, R., 2005. How does transcranial DC stimulation of the primary motor cortex alter regional neuronal activity in the human brain? Eur. J. Neurosci. 22, 495–504.

Li, C.-S.R., Yan, P., Bergquist, K.L., Sinha, R., 2007. Greater activation of the "default" brain regions predicts stop signal errors. NeuroImage 38, 640–648.

Mason, M.F., Norton, M.I., Van Horn, J.D., Wegner, D.M., Grafton, S.T., Macrae, C.N., 2007. Wandering minds: the default network and stimulus-independent thought. Science 315, 393–395.

Nichols, T.E., Holmes, A.P., 2002. Nonparametric permutation tests for functional neuroimaging: a primer with examples. Hum. Brain Mapp. 15, 1–25.

Nitsche, M., Paulus, W., 2000. Excitability changes induced in the human motor cortex by weak transcranial direct current stimulation. J. Physiol. 527, 633–639.

Nitsche, M.A., Seeber, A., Frommann, K., Klein, C.C., Rochford, C., Nitsche, M.S., Fricke, K., Liebetanz, D., Lang, N., Antal, A., Paulus, W., Tergau, F., 2005. Modulating parameters of excitability during and after transcranial direct current stimulation of the human motor cortex. J. Physiol. Lond. 568, 291–303.

Peña-Gómez, C., Sala-Lonch, R., Junqué, C., Clemente, I.C., Vidal, D., Bargalló, N., Falcón, C., Valls-Sole, J., Pascual-Leone, A., Bartrés-Faz, D., 2012. Modulation of large-scale brain networks by transcranial direct current stimulation evidenced by resting-state functional MRI. Brain Stimul. 5, 252–263.

Polanía, R., Paulus, W., Antal, A., Nitsche, M.A., 2011. Introducing graph theory to track for neuroplastic alterations in the resting human brain: a transcranial direct current stimulation study. NeuroImage 54, 2287–2296.

Polanía, R., Paulus, W., Nitsche, M.A., 2012a. Reorganizing the intrinsic functional architecture of the human primary motor cortex during rest with non-invasive cortical stimulation. PLoS ONE 7, e30971.

Polanía, R., Paulus, W., Nitsche, M.A., 2012b. Modulating cortico-striatal and thalamo-cortical functional connectivity with transcranial direct current stimulation. Hum. Brain Mapp. 33, 2499–2508.

Raichle, M.E., MacLeod, A.M., Snyder, A.Z., Powers, W.J., Gusnard, D.A., Shulman, G.L., 2001. A default mode of brain function. Proc. Natl. Acad. Sci. U. S. A. 98, 676–682.

Rosazza, C., Minati, L., 2011. Resting-state brain networks: literature review and clinical applications. Neurol. Sci. 32, 773–785.

Rosenkranz, K., Nitsche, M., Tergau, F., Paulus, W., 2000. Diminution of training-induced transient motor cortex plasticity by weak transcranial direct current stimulation in the human. Neurosci. Lett. 296, 61–63.

Sehm, B., Kipping, J., Schäfer, A., Villringer, A., Ragert, P., 2013. A comparison between uni- and bilateral tDCS effects on functional connectivity of the human motor cortex. Front. Hum. Neurosci. 7, 183.

Sehm, B., Schafer, A., Kipping, J., Margulies, D., Conde, V., Taubert, M., Villringer, A., Ragert, P., 2012. Dynamic modulation of intrinsic functional connectivity by transcranial direct current stimulation. J. Neurophysiol. 108, 3253–3263.

Smith, Stephen, Jenkinson, M., Woolrich, M., Beckmann, C., Behrens, T., Johansen-Berg, H., Bannister, P., De Luca, M., Drobnjak, I., Flitney, D., Niazy, R., Saunders, J., Vickers, J., Zhang, Y., De Stefano, N., Brady, J., Matthews, P., 2004. Advances in functional and structural MR image analysis and implementation as FSL. NeuroImage 23, S208–S219.

Smith, S.M., Fox, P.T., Miller, K.L., Glahn, D.C., Fox, P.M., Mackay, C.E., Filippini, N., Watkins, K.E., Toro, R., Laird, A.R., Beckmann, C., 2009. Correspondence of the brain's functional architecture during activation and rest. Proc. Natl. Acad. Sci. USA 106, 13040–13045.

Sonuga-Barke, E.J.S., Castellanos, F.X., 2007. Spontaneous attentional fluctuations in impaired states and pathological conditions: a neurobiological hypothesis. Neurosci. Biobehav. Rev. 31, 977–986.

Stagg, C.J., Bachtiar, V., Johansen-Berg, H., 2011a. The role of GABA in human motor learning. Curr. Biol. 1–5.

Stagg, C.J., Best, J.G., Stephenson, M.C., O'Shea, J., Wylezinska, M., Kincses, Z.T., Morris, P.G., Matthews, P.M., Johansen-Berg, H., 2009a. Polarity-sensitive modulation of cortical neurotransmitters by transcranial stimulation. J. Neurosci. 29, 5202–5206.

Stagg, C.J., Jayaram, G., Pastor, D., Kincses, Z.T., Matthews, P.M., Johansen-Berg, H., 2011b. Polarity and timing-dependent effects of transcranial direct current stimulation in explicit motor learning. Neuropsychologia 49, 800–804.

Stagg, C.J., Lin, R.L., Mezue, M., Segerdahl, A., Kong, Y., Xie, J., Tracey, I., 2013. Widespread modulation of cerebral perfusion induced during and after transcranial direct current stimulation applied to the left dorsolateral prefrontal cortex. J. Neurosci. 33, 11425–11431.

Stagg, C.J., O'Shea, J., Kincses, Z.T., Woolrich, M., Matthews, P.M., Johansen-Berg, H., 2009b. Modulation of movement-associated cortical activation by transcranial direct current stimulation. Eur. J. Neurosci. 30, 1412–1423.

Stagg, C.J.C., Bachtiar, V.V., O'Shea, J.J., Allman, C.C., Bosnell, R.A.R., Kischka, U.U., Matthews, P.M.P., Johansen-Berg, H.H., 2012. Cortical activation changes underlying stimulation-induced behavioural gains in chronic stroke. Brain 135, 276–284.

Venkatakrishnan, A., Contreras-Vidal, J.L., Sandrini, M., Cohen, L.G., 2011. Independent component analysis of resting brain activity reveals transient modulation of local cortical processing by transcranial direct current stimulation. Presented at the 2011 33rd Annual International Conference of the IEEE Engineering in Medicine and Biology Society, IEEE, pp. 8102–8105.

Weissman, D.H., Roberts, K.C., Visscher, K.M., Woldorff, M.G., 2006. The neural bases of momentary lapses in attention. Nat. Neurosci. 9, 971–978.

Woolrich, M.W., Jbabdi, S., Patenaude, B., Chappell, M., Makni, S., Behrens, T., Beckmann, C., Jenkinson, M., Smith, S.M., 2009. Bayesian analysis of neuroimaging data in FSL. NeuroImage 45.

Woolrich, M.W., Ripley, B.D., Brady, M., Smith, S.M., 2001. Temporal autocorrelation in univariate linear modeling of FMRI data. NeuroImage 14, 1370–1386.